

ChemComm

Accepted Manuscript



This article can be cited before page numbers have been issued, to do this please use: W. Zuo, Z. Huang, Y. Zhao, W. Xu, Z. Liu, X. Yang, C. Jia and B. Wu, *Chem. Commun.*, 2018, DOI: 10.1039/C8CC03883J.



This is an Accepted Manuscript, which has been through the Royal Society of Chemistry peer review process and has been accepted for publication.

Accepted Manuscripts are published online shortly after acceptance, before technical editing, formatting and proof reading. Using this free service, authors can make their results available to the community, in citable form, before we publish the edited article. We will replace this Accepted Manuscript with the edited and formatted Advance Article as soon as it is available.

You can find more information about Accepted Manuscripts in the [author guidelines](#).

Please note that technical editing may introduce minor changes to the text and/or graphics, which may alter content. The journal's standard [Terms & Conditions](#) and the ethical guidelines, outlined in our [author and reviewer resource centre](#), still apply. In no event shall the Royal Society of Chemistry be held responsible for any errors or omissions in this Accepted Manuscript or any consequences arising from the use of any information it contains.

Chirality sensing of choline derivatives by a triple anion helicate cage through induced circular dichroism

Received 00th January 20xx,
Accepted 00th January 20xx

Wei Zuo, Zhe Huang, Yanxia Zhao, Wenhua Xu, Zhihua Liu, Xiao-Juan Yang, Chuandong Jia,* and Biao Wu*

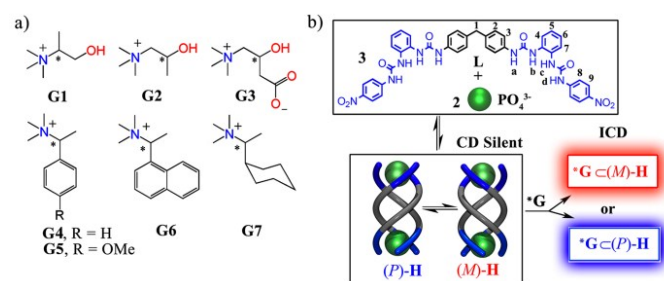
DOI: 10.1039/x0xx00000x

www.rsc.org/

Chirality sensing of choline derivatives is achieved by a self-assembled, racemic triple anion helicate cage which exhibits induced circular dichroism (ICD) upon encapsulation of a chiral guest. The host-guest interactions were illustrated by NMR, crystal structure, CD and DFT calculations. The absolute configurations and ee values were determined by ICD.

Choline and its derivatives, such as acetylcholine, methylcholine and carnitine, play important roles in biological systems.¹ When the molecule is chiral, the biological activity is closely related to its chirality. For examples, *R*(+)- α -methylcholine and *S*(+)- β -methylcholine (Scheme 1a, (*R*)-**G1**, (*S*)-**G2**) are significantly better inhibitors of the high-affinity choline transport system than their enantiomers.² *L*-carnitine (Scheme 1a, (*R*)-**G3**) has important pharmacological and nutritional functions and is used as a drug for the therapy of dislipoproteinemia, anorexia, and dyspepsia, while *D*-carnitine is harmful to human health.^{3,4} Therefore, it is essential to determine the enantiomeric purity of these biomolecules.

Chirality sensing is commonly realized by chiral chromatography, NMR spectroscopy and various optical methods.⁵ The circular dichroism (CD) is especially attractive because of such advantages as simultaneous determination of both of the absolute configuration and enantiomeric excess (ee) values, and concentration-independent spectral response.⁶ However, since many chiral species lack a strong chromophoric group, direct chirality sensing by CD is not applicable. Alternatively, these CD-silent analytes, such as amines, alcohols, amino alcohols, amino acids, carboxylic acids and epoxides are generally sensed by induced circular dichroism (ICD) of reporter molecules which are held nearby



Scheme 1. (a) Structures of chiral quaternary ammonium ions **G1–G7** (cations were used as PF_6^- salts) (b) The proposed host-guest system for chirality sensing of quaternary ammonium ions with the triple anion helicate host, $[(\text{PO}_4)_2\text{L}_3]^{6-}$ (**H**).

via a dynamic covalent (derivation system)⁷ or noncovalent binding event (host-guest system), such as metal coordination,⁸ hydrogen bonding,⁹ hydrophobic effect,¹⁰ and $\pi\cdots\pi$ stacking.¹¹

Determination of the enantiomeric purity of some chiral quaternary ammonium ions (including **G3**, **G4** and **G6**) was achieved by NMR spectroscopy using chiral macrocycles or counter anions as the chiral shift agents.¹² The ICD method was employed to detect the absolute configuration **G4** and **G6** by achiral hosts such as *p*-sulfonatocalix[n]arenes^{10c} or a single helical resorcinol oligomer.^{11b} However, chirality sensing of α -/ β -methylcholine (**G1**, **G2**) and carnitine (**G3**) through ICD has not been reported yet. We recently reported a triple anion helicate cage, $[(\text{PO}_4)_2\text{L}_3]^{6-}$ (**H**, host), which features a biomimetic aromatic box capable of binding choline and acetylcholine through cation- π and electrostatic interactions.¹³ Considering the inherent chirality and guest encapsulation ability of **H**, we set to exploit its possible use for sensing chiral choline analogues.

Though there is no chiral ligand in the triple helicate structure of **H**, supramolecular chirality¹⁴ is encoded through nonsymmetric arrangement of the ligands. In the absence of guests, the host **H** exists as a racemic mixture of *P* and *M* conformers and is thus CD silent. When encapsulating a chiral (non-racemic) guest, due to the different binding affinities, the balance between *P* and *M* conformers will be broken and the

Key Laboratory of Synthetic and Natural Functional Molecule Chemistry of the Ministry of Education, College of Chemistry and Materials Science, Northwest University, Xi'an 710069 (China).

E-mail: jcd2015@nwu.edu.cn (C.J.); wubiao@nwu.edu.cn (B.W.)

† Electronic Supplementary Information (ESI) available: Synthetic procedures, characterization and computations (PDF), and corresponding CIF files (CIF). CCDC 1815936. For ESI and crystallographic data in CIF or other electronic format see DOI:10.1039/x0xx00000x

supramolecular chirality is expressed as either *P* or *M* (ICD signals), thus enabling the chirality detection. Herein we report the ICD-based studies on host **H** with choline derivatives, including determination of the absolute configuration, association constants, and ee values. Without the requirement of guest-derivation, this host-guest system enables real-time monitor of guest chirality. To elucidate the influence of substituents on the chirality sensing, seven pairs of analytes were examined, including α -methylcholine (**G1**), β -methylcholine (**G2**), *D,L*-carnitine (**G3**) and analogues with phenyl-, naphthyl-, and cyclohexyl groups (**G4–G7**) (Scheme 1).

^1H NMR spectra (400 MHz, $\text{MeCN-}d_3$) reveal the binding of **H** toward the guests $\pm\text{G1–G7}$ by upfield shifts of the ' Me_3N^+ ' signals ($\Delta\delta_{\text{H}\alpha} = -0.4$ to -2.5 ppm compared with free guests), which is a clear indication of encapsulation of the trimethylammonium head of the guest in the aromatic box of **H** (Figs. 1a and S21–26).¹³ As estimated by the upfield shifts, $\pm\text{G2}$ ($\Delta\delta_{\text{H}\alpha} = -2.5$ ppm) and $\pm\text{G1}$ ($\Delta\delta_{\text{H}\alpha} = -2.3$ ppm) showed the strongest binding, followed by $\pm\text{G5}$ ($\Delta\delta_{\text{H}\alpha} = -1.4$ ppm), $\pm\text{G4}$ ($\Delta\delta_{\text{H}\alpha} = -1.2$ ppm), $\pm\text{G7}$ ($\Delta\delta_{\text{H}\alpha} = -0.9$ ppm), $\pm\text{G6}$ ($\Delta\delta_{\text{H}\alpha} = -0.7$ ppm) and $\pm\text{G3}$ ($\Delta\delta_{\text{H}\alpha} = -0.4$ ppm).

In the case of $\pm\text{G1}$, guest encapsulation was further supported by the crystal structure of the complex $(\text{TBA})_5[(\pm\text{G1})\text{C}(\text{PO}_4)_2\text{L}_3]$ ($\pm\text{G1C}\cdot\text{H}$; TBA = tetrabutylammonium), which is composed of equal amounts of (*R*)-**G1C**(*M*)-**H** and (*S*)-**G1C**(*P*)-**H**, indicating the enantioselective binding of (*R*)-**G1** and (*S*)-**G1** by (*M*)-**H** and (*P*)-**H**, respectively (Fig. 1b). The trimethylammonium head of $\pm\text{G1}$ is included in the 'aromatic box' of **H** through electrostatic and cation– π interactions¹⁵ (blue dashed lines, $\text{N}\cdots\text{centroid}$ distances: 4.467–5.573 Å, average 4.810 Å, Fig. S27). The methyl group (H_γ , Fig. 1a) of $\pm\text{G1}$ forms $\text{CH}\cdots\pi$ interaction with one phenyl group of **H** ($\text{C}\cdots\text{centroid}$ distance: 3.686 Å, Fig. S27). Notably, the hydroxyl tail of $\pm\text{G1}$ is also located inside the cage and donates a hydrogen bond to one oxygen atom of a phosphate ion ($\text{O}\cdots\text{O} = 2.887$ Å, $\angle\text{OHO} = 170^\circ$).

The ^1H NMR results of $\pm\text{G1C}\cdot\text{H}$ (TBA^+ as the counteranion, Fig. 1a) match well with the crystal structure. Upon encapsulation by **H**, the signals of H_α ($\Delta\delta = -2.3$ ppm), H_β ($\Delta\delta = -3.2$ ppm) and H_γ ($\Delta\delta = -2.3$ ppm) of $\pm\text{G1}$ all display significant upfield shifts (that of the methylene H_χ could not be assigned due to signals overlap), demonstrating the shielding effect imposed by the aromatic cage. The OH signal shows a large downfield shift ($\Delta\delta = 2.8$ ppm), while the urea NHa signal of host **H** shifts back to upfield by -1.0 ppm (see Scheme 1a for proton numbering). These changes are consistent with the hydrogen bonding interaction between OH ($\pm\text{G1}$) and one coordinated PO_4^{3-} (the interaction with hydroxyl weakens the binding of PO_4^{3-} with NHa). The 2D NMR spectra of $\pm\text{G1C}\cdot\text{H}$ show strong NOE correlations between OH ($\pm\text{G1}$)/NHa-c (**H**) and Me_3N^+ ($\pm\text{G1}$)/H2 (**H**) (Fig. S28–S32). Additionally, HRMS studies confirmed the formation of a complex with the stoichiometry $[(\text{PO}_4)_2\text{L}_3(\pm\text{G1})]$ ($[(\text{PO}_4)_2\text{L}_3(\pm\text{G1})(\text{TBA})_3]^{2-}$, obsd. 1709.8159 vs calcd. 1709.8288, Fig. S34).

It should be mentioned that the dual-site binding mode of $\pm\text{G1}$ (α -methylcholine) presented herein prompts us to

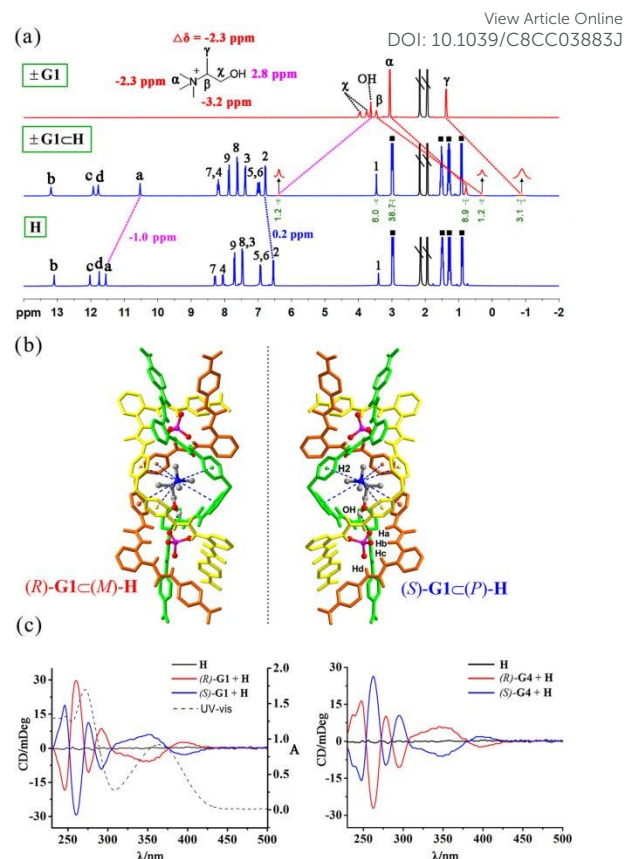


Fig. 1 (a) ^1H NMR spectra (400 MHz, $\text{MeCN-}d_3$) of $\pm\text{G1}$, $\pm\text{G1C}\cdot\text{H}$ and **H** (Insets: enlarged proton signals). (b) X-ray single-crystal structures of $\pm\text{G1C}\cdot\text{H}$, showing enantiomers of (*R*)-**G1C**(*M*)-**H** and (*S*)-**G1C**(*P*)-**H** (counter cations, solvent molecules, and non-acidic protons are omitted for clarity). (c) UV-vis spectrum (dotted line) and CD spectra of **H** (10 μM , MeCN) before and after addition of one equiv. of enantiomers of **G1** and **G4**.

reconsider the proposed binding mode of choline (Ch) in our previous studies.¹³ Based on the DFT optimized structure of $\text{Ch}\cdot\text{H}$, it was assumed that the Me_3N^+ head was encapsulated in the aromatic box of **H** while the hydroxyl tail was bound in the outside by two urea oxygen atoms (instead of by PO_4^{3-} ion as observed for $\pm\text{G1}$). A comparison of the ^1H NMR spectra of complexes $\text{Ch}\cdot\text{H}$ and $\pm\text{G1C}\cdot\text{H}$ reveals almost same features (except that the OH signal of Ch could not be assigned due to severe broadening, Fig. S35). Large upfield shift of Me_3N^+ of Ch ($\Delta\delta = -2.4$ ppm) and downfield shift of NHa of **H** ($\Delta\delta = 1.0$ ppm) were observed, implying that the hydroxyl tail of Ch is possibly bound by the phosphate ion rather than by urea oxygen atoms. To further elucidate this issue, DFT computations were carried out on $\text{Ch}\cdot\text{H}$. Both binding modes for OH group (Model I, with phosphate ion; Model II, with two urea oxygen atoms; Fig. S36) were optimized, with the mode I being more energetically favored by 9.72 kcal mol^{-1} (Table S2).

Since the crystal structure of $\pm\text{G1C}\cdot\text{H}$ reveals enantioselective binding of (*R*)-**G1** and (*S*)-**G1** by (*M*)-**H** and (*P*)-**H**, respectively, it is reasonable to assume that the binding of a chiral (non-racemic) guest would induce enhanced population of (*M*)-**H** or (*P*)-**H**, and thus allows detection of the ICD signals of **H**, which is correlated with the guest chirality. With this in mind, chirality sensing of guests $\pm\text{G1–G7}$ by **H** was

investigated by CD measurements. Either **H** or enantiomers of $\pm\mathbf{G1}\text{--}\pm\mathbf{G7}$ do not show obvious signals throughout the tested wavelength range (230–500 nm, Fig. 1c, S38) in MeCN. However, with addition of 1.0 equiv of an enantiomer of guest to the solution of **H** (10 μM), strong Cotton effects (three positive, three negative) were observed in the region where **H** absorbs (230–450 nm, Fig. 1c, see UV-Vis spectrum of **H**). All guests induced similarly shaped CD spectra and each pair of enantiomers induced perfectly mirror imaged spectra (Fig. 1c, S39). Noticeably, $\pm\mathbf{G1}\text{--}\pm\mathbf{G3}$ and $\pm\mathbf{G4}\text{--}\pm\mathbf{G7}$ induced contrary chirality correlation between the guest's chirality (*R* or *S*) and the host's helicity (*P* or *M*). For example, the CD spectrum of **H** and (*R*)-**G1** shows a maximum positive Cotton effect at $\lambda_{\text{max}} = 261$ nm, while addition of (*R*)-**G4** caused one negative Cotton effect at $\lambda_{\text{max}} = 262$ nm (Fig. 1c). According to the crystal structure of $\mathbf{G1}\subset\mathbf{H}$ (Fig. 1b), (*R*)-**G1** prefers to be bound by (*M*)-**H** and the induced helicity was assigned as *M*. In contrast, the helicity induced by (*R*)-**G4** was *P*. Consistently, DFT calculations indicated that the optimized structure of (*R*)-**G4** \subset (*P*)-**H** is 10.7 kcal mol⁻¹ lower in energy than (*R*)-**G4** \subset (*M*)-**H** (Fig. S37 and Table S3).

The association constants between **H** and enantiomers of $\mathbf{G1}\text{--}\mathbf{G7}$ were determined by CD titrations. Following incremental addition of a chiral guest to **H**, the CD signals gradually increased till reaching saturation (Fig. S40, Table 1). The appearance of clear isodichroic points at 252, 270, 284, 304, 377 nm suggests that the equilibrium involves a single stoichiometric relationship between **H** and **G**, which was determined as 1:1 by the Job's plot (Fig. S41). The intensity of the strongest CD signal (θ) for $\mathbf{G1}\text{--}\mathbf{G7}$ at $\lambda_{\text{max}} = 259\text{--}262$ nm (Table 1) was plotted against the concentration of a guest enantiomer, and the titration profiles were subjected to least-squares nonlinear fitting to a 1:1 binding model by Dynafit program.¹⁶ As shown in Table 1, each pair of enantiomers shows almost the same association constant and the selectivity of **H** for the tested guests is in the order $\pm\mathbf{G2} > \pm\mathbf{G1} > \pm\mathbf{G5} > \pm\mathbf{G6} > \pm\mathbf{G4} > \pm\mathbf{G7} > \pm\mathbf{G3}$. This tendency is consistent with the NMR results except that the binding affinity of $\pm\mathbf{G6}$ was

Table 1 Guest encapsulation induced host helicities, θ_{max} (mDeg)/ λ (nm), and association constants (K_a , M⁻¹) of **H** to $\mathbf{G1}\text{--}\mathbf{G7}$.

Guest	Induced helicity	θ_{max} (mDeg)/ λ (nm)	K_a /M ⁻¹
(<i>R</i>)- G1	<i>M</i>	+36/261	1.18×10^6
(<i>S</i>)- G1	<i>P</i>	-37/261	1.16×10^6
(<i>R</i>)- G2	<i>M</i>	+39/261	1.88×10^6
(<i>S</i>)- G2	<i>P</i>	-40/261	1.78×10^6
(<i>R</i>)- G3	<i>M</i>	+42/259	1.57×10^4
(<i>S</i>)- G3	<i>P</i>	-43/259	1.50×10^4
(<i>R</i>)- G4	<i>P</i>	-52/262	1.75×10^5
(<i>S</i>)- G4	<i>M</i>	+53/262	1.86×10^5
(<i>R</i>)- G5	<i>P</i>	-59/262	3.31×10^5
(<i>S</i>)- G5	<i>M</i>	+57/262	3.29×10^5
(<i>R</i>)- G6	<i>P</i>	-20/261	2.11×10^5
(<i>S</i>)- G6	<i>M</i>	+20/261	2.21×10^5
(<i>R</i>)- G7	<i>P</i>	-22/259	4.82×10^4
(<i>S</i>)- G7	<i>M</i>	+23/259	4.91×10^4

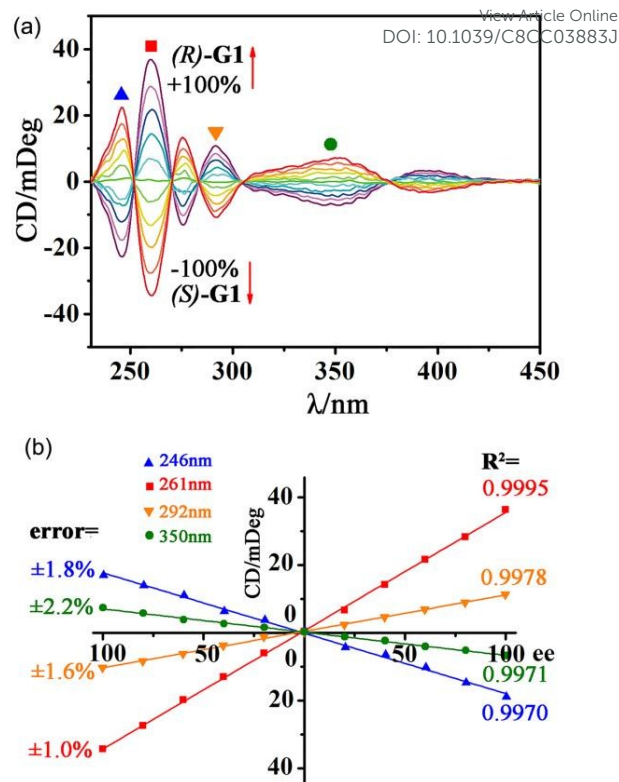


Fig. 2 (a) CD spectra of **H** (10 μM , MeCN) in the presence of 2 equiv. of **G1** with various ee values, and (b) the corresponding ee calibration plots at 246, 261, 292 and 350 nm.

underestimated. Upon formation of the host-guest complex, $\pm\mathbf{G1}$ and $\pm\mathbf{G2}$ show larger changes of the chemical shifts than $\pm\mathbf{G4}\text{--}\pm\mathbf{G7}$ due to the dual-site binding of both of the Me_3N^+ head and OH tail. The charge neutral zwitterion $\pm\mathbf{G3}$ displays the smallest K_a which is reasoned by the lack of electrostatic interactions with the host **H**. The stronger binding of $\pm\mathbf{G6}$ than $\pm\mathbf{G4}$ may be attributed to the stronger $\pi\cdots\pi$ interactions of the aryl tail of the guest with the host, which is indicated by the upfield shifts of the guest's phenyl protons in the ¹H NMR spectra of $\pm\mathbf{G}\subset\mathbf{H}$ (Fig. S23–24 and S26). Finally, the weaker binding of the cyclohexyl-functionalized $\pm\mathbf{G7}$ can be attributed to both the larger steric effect and the lack of an aromatic tail.

To evaluate the possibility of fast ee determination, CD spectra of **H** were collected in the presence of $\mathbf{G1}\text{--}\mathbf{G7}$ with varying enantiomeric compositions (Figs. 2a and S42). Saturated equivalents of the analytes were used to ensure concentration-independent spectral responses. For a typical instance, the CD intensity of **H** was plotted against the %ee value of **G1** at 246, 261, 292, 350 nm, which consistently showed linear relationship ($R^2 = 0.9995\text{--}0.9970$, Fig. 2b). CD spectra of five “unknown” solutions of **G1** were recorded and the average errors were calculated. The lowest value, $\pm 1\%$, was obtained at 261 nm (Fig 2b). Accordingly, the strongest CD signal at $\lambda_{\text{max}} = 259\text{--}262$ nm (Table 1) was selected to determinate the ee values of $\pm\mathbf{G2}\text{--}\pm\mathbf{G7}$, with acceptable average errors of $\pm 1.0\%\text{--}\pm 1.8\%$ (Fig. S42 and Table S4).^{8c}

In conclusion, a self-assembled triple anion helicate cage is capable of encapsulating chiral choline analogues to generate strong ICD signals, which enables a real-time CD screening

system for determination of the absolute configurations, ee values and association constants. The presented example combines the advantage of self-assembly of a complex host (triple helicate cage) from simple, inexpensive starting materials, and that of noncovalent host-guest interactions for instant chirality sensing without the requirement of derivatization. Further exploration of the application of such anion-based cages in chirality recognition is underway.

Acknowledgements

We are grateful to the financial supports of National Natural Science Foundation of China (21701132, 21772154 and 21325102), Education Department of Shaanxi (16JS113), Northwest University (2018212) and China Postdoctoral Science Foundation (2016M602849).

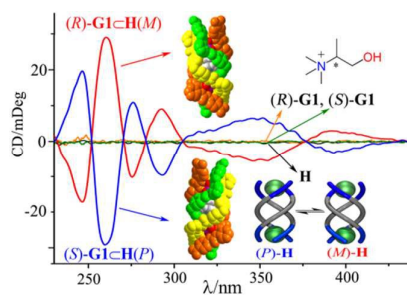
Conflicts of interest

There are no conflicts to declare.

Notes and references

- (a) D. D. Allen and P. R. Lockman, *Life Sci.*, 2003, **73**, 1609–1615; (b) P. H. N. Celie, S. E. v. Rossum-Fikkert, W. J. v. Dijk, K. Brejc, A. B. Smit and T. K. Sixma, *Neuron*, 2004, **41**, 907–914; (c) G. Jogl and L. Tong, *Cell*, 2003, **112**, 113–122; (d) A. Karlin, *Nat. Rev. Neurosci.*, 2002, **3**, 102–114.
- S. S. G. Ferguson, M. Diksic and B. Collier, *J. Neurochem.*, 1991, **57**, 915–921.
- J. D. McGarry and N. F. Brown, *Eur. J. Biochem.*, 1997, **244**, 1–14.
- (a) L. Sánchez-Hernández, M. Castro-Puyana, C. García-Ruiz, A. L. Crego and M. L. Marina, *Food Chem.*, 2010, **120**, 921–928; (b) L. Sánchez-Hernández, C. García-Ruiz, A. L. Crego and M. L. Marina, *J. Pharm. Biomed. Anal.*, 2010, **53**, 1217–1223.
- (a) L. You, D. Zha and E. V. Anslyn, *Chem. Rev.*, 2015, **115**, 7840–7892; (b) D. Leung, S. O. Kang and E. V. Anslyn, *Chem. Soc. Rev.*, 2012, **41**, 448–479; (c) J. Dong, C. Tan, K. Zhang, Y. Liu, P. J. Low, J. Jiang and Y. Cui, *J. Am. Chem. Soc.*, 2017, **139**, 1554–1564; (d) W. Xuan, M. Zhang, Y. Liu, Z. Chen and Y. Cui, *J. Am. Chem. Soc.*, 2012, **134**, 6904–6907.
- (a) L. Pu, *Acc. Chem. Res.*, 2017, **50**, 1032–1040; (b) L. Pu, *Chem. Rev.*, 2004, **104**, 1687–1171; (c) X. Zhang, J. Yin and J. Yoon, *Chem. Rev.*, 2014, **114**, 4918–4959; (d) H. H. Jo, C.-Y. Lin and E. V. Anslyn, *Acc. Chem. Res.*, 2014, **47**, 2212–2221.
- (a) Z. Chen, Q. Wang, X. Wu, Z. Li and Y.-B. Jiang, *Chem. Soc. Rev.*, 2015, **44**, 4249–4263; (b) C. Wolf and K. W. Bentley, *Chem. Soc. Rev.*, 2013, **42**, 5408–5424; (c) C. Ni, D. Zha, H. Ye, Y. Hai, Y. Zhou, E. Anslyn and L. You, *Angew. Chem. Int. Ed.*, 2018, **1300**–1305; (d) F. Y. Thanzeel and C. Wolf, *Angew. Chem. Int. Ed.*, 2017, **56**, 7276–7281; (e) S. L. Pilicer, P. R. Bakhshi, K. W. Bentley and C. Wolf, *J. Am. Chem. Soc.*, 2017, **139**, 1758–1761; (f) S. L. Pilicer, P. R. Bakhshi, K. W. Bentley and C. Wolf, *J. Am. Chem. Soc.*, 2017, **139**, 1758–1761; (g) C.-Y. Lin, M. W. Giuliano, B. D. Ellis, S. J. Miller and E. V. Anslyn, *Chem. Sci.*, 2016, **7**, 4085–4090; (h) Z. A. De los Santos and C. Wolf, *J. Am. Chem. Soc.*, 2016, **138**, 13517–13520; (i) X.-X. Chen, Y.-B. Jiang and E. V. Anslyn, *Chem. Commun.*, 2016, **52**, 12669–12671; (j) J.-B. Xiong, H.-T. Feng, J.-P. Sun, W.-Z. Xie, D. Yang, M. Liu and Y.-S. Zheng, *J. Am. Chem. Soc.*, 2016, **138**, 11469–11472.
- (a) K. W. Bentley, P. Zhang and C. Wolf, *Sci. Adv.*, 2016, **2**, e1501162; (b) X. Li, C. E. Burrell, R. J. Staples and B. Borhan, *J. Am. Chem. Soc.*, 2012, **134**, 9026–9029; (c) L. A. Joyce, M. S. Maynor, J. M. Dragna, G. M. da Cruz, V. M. Lynch, J. W. Canary and E. V. Anslyn, *J. Am. Chem. Soc.*, 2011, **133**, 13746–13752; (d) S. J. Wezenberg, G. Salassa, E. C. Escudero-Adán, J. Benet-Buchholz and A. W. Kleij, *Angew. Chem. Int. Ed.*, 2011, **50**, 713–716; (e) G. Proni, G. Pescitelli, X. Huang, K. Nakanishi and N. Berova, *J. Am. Chem. Soc.*, 2003, **125**, 12914–12927; (f) H. Tsukube and S. Shinoda, *Chem. Rev.*, 2002, **102**, 2389–2403; (g) X. Huang, B. H. Rickman, B. Borhan, N. Berova and K. Nakanishi, *J. Am. Chem. Soc.*, 1998, **120**, 6185–6186; (h) X. Huang, B. H. Rickman, B. Borhan, N. Berova and K. Nakanishi, *J. Am. Chem. Soc.*, 1995, **117**, 7021–7022; (i) *J. Am. Chem. Soc.*, 1995, **117**, 7021–7022.
- (a) M. Hasan, V. N. Khose, A. D. Pandey, V. Borovkov and A. V. Karnik, *Org. Lett.*, 2016, **18**, 440–443; (b) Y. Ishii, Y. Onda and Y. Kubo, *Tetrahedron Lett.*, 2006, **47**, 8221–8225; (c) M. Inouye, M. Waki and H. Abe, *J. Am. Chem. Soc.*, 2004, **126**, 2022–2027; (d) T. Mizutani, H. Takagi, O. Hara, T. Horiguchi and H. Ogoshi, *Tetrahedron Lett.*, 1997, **38**, 1991–1994; (e) M. Anyika, H. Gholami, K. D. Ashtekar, R. Acho and B. Borhan, *J. Am. Chem. Soc.*, 2014, **136**, 550–553; (f) H. Gholami, M. Anyika, J. Zhang, C. Vasileiou and B. Borhan, *Chem. Eur. J.*, 2016, **22**, 9235–9239; (g) M. J. Kim, Y. R. Choi, H.-G. Jeon, P. Kang, M.-G. Choi and K.-S. Jeong, *Chem. Commun.*, 2013, **49**, 11412–11414.
- (a) L.-L. Wang, Z. Chen, W.-E. Liu, H. Ke, S.-H. Wang and W. Jiang, *J. Am. Chem. Soc.*, 2017, **139**, 8436–8439; (b) R. B. Prince, S. A. Barnes and J. S. Moore, *J. Am. Chem. Soc.*, 2000, **122**, 2758–2762; (c) T. Morozumi and S. Shinkai, *J. Chem. Soc. Chem. Commun.*, 1994, 1219–1220.
- (a) Y. Tsunoda, K. Fukuta, T. Imamura, R. Sekiya, T. Furuyama, N. Kobayashi and T. Haino, *Angew. Chem., Int. Ed.*, 2014, **53**, 7243–7247; (b) H. Goto, Y. Furusho and E. Yashima, *Chem. Commun.*, 2009, 1650–1652; (c) F. Biedermann and W. M. Nau, *Angew. Chem. Int. Ed.*, 2014, **53**, 5694–5699.
- (a) G.-W. Zhang, P.-F. Li, Z. Meng, H.-X. Wang, Y. Han and C.-F. Chen, *Angew. Chem. Int. Ed.*, 2016, **55**, 5304–5308; (b) J. R. Cochrane, A. Schmitt, U. Wille and C. A. Hutton, *Chem. Commun.*, 2013, **49**, 8504–8506; (c) M. A. Petti, T. J. Shepodd, J. Richard E. Barrans and D. A. Dougherty, *J. Am. Chem. Soc.*, 1988, **110**, 6825–6840; (d) M. E. Amato, F. P. Ballistreri, S. Gentile, A. Pappalardo, G. A. Tomaselli and R. M. Toscano, *J. Org. Chem.*, 2010, **75**, 1437–1443; (e) K. Ito, M. Noike, A. Kida and Y. Ohba, *J. Org. Chem.*, 2002, **67**, 7519–7522; (f) J. Lacour, L. Vial and C. Herse, *Org. Lett.*, 2002, **4**, 1351–1354.
- C. Jia, W. Zuo, X.-J. Yang, Y. Chen, D. Yang, L. Cao, R. Custelcean, J. Hostaš, P. Hobza, R. Glaser and B. Wu, *Nat. Commun.*, 2017, **8**, 938.
- (a) E. Yashima, N. Ousaka, D. Taura, K. Shimomura, T. Ikai and K. Maeda, *Chem. Rev.*, 2016, **116**, 13752–13990; (b) M. Liu, L. Zhang and T. Wang, *Chem. Rev.*, 2015, **115**, 7304–7397; (c) M. A. Mateos-Timoneda, M. Crego-Calama and D. N. Reinhoudt, *Chem. Soc. Rev.*, 2004, **33**, 363–372.
- (a) D. A. Dougherty, *Acc. Chem. Res.*, 2013, **46**, 885–893; (b) A. S. Mahadevi and G. N. Sastry, *Chem. Rev.*, 2013, **113**, 2100–2138.
- P. Kuzmič, *Anal. Biochem.*, 1996, **237**, 260–273.

TOC



A racemic A_2L_3 triple anion helicate cage is able to sense chiral choline derivatives by induced circular dichroism.